OS51F-1313

A New Procedure for Quick Estimation of Porosity and Density of Hydrate-bearing Sediments by Using Medical X-ray CT Scanner

L. P. Gupta[1], W. Tanikawa[1], Y. Hamada[1], T. Hirose[1], N. Ahagon[1], T. Sugihara[2], N. Abe[3], S. Nomura[4], Y. Masaki[5], H.-Yu Wu[3], W. Lin[6], M. Kinoshita[7] and Y. Yamada[3]
and NGHP Expedition 02 JAMSTEC Science Team

[1]KOCHI, JAMSTEC, Nankoku, Japan, [2]CDEX, [3]ODS, [4]MAT, JAMSTEC, Yokohama, Japan, [5]CSR, JAMSTEC, Yokosuka, Japan, [6]Dept. Urban Managament, Kyoto University, Japan, [7]ERI, The University of Tokyo, Japan

Abstract

Gas hydrates start decomposing soon after recovery of host sediments through coring operations due to changes in ambient pressure and temperature. This decomposition leads to changes in sedimentary structures that may complicate physical property related measurements of the sediments by time-consuming conventional methods. In this study, we used a medical X-ray CT scanner to quickly scan the cored sediments, and used raw data (CT numbers), and thus avoided image processing steps, to estimate porosity and density of the sediments. The raw data were obtained by drawing a circular region of interest (ROI) to cover most of the sediments visible in a cross section XCT image of the sediments. The data were weighted for relative contribution of liquid and solid in sediments before estimating porosity. On the other hand, density was estimated by using an average CT number that was automatically calculated by the Osirix software used for drawing the ROI, and by using an XCT - density calibration equation. Although some uncertainty in estimation of relative volumes of solid, liquid and gas could not be avoided, the results obtained by this new procedure were in good agreement with those obtained by conventional methods.

Instrument

Deep sea hydrate-bearing sediments from Bay of Bengal were scanned soon after recovery onboard drillship Chikyu by using a medical X-ray CT scanner (GE Discovery CT750 HD system). The CT images of the sediment show obvious sign of hydrates.

Scientifc drilling ship "Chikyu"

Core section processing onboard Chikyu

Core being retrieved on Chikyu

XCT scanner onboard Chikyu

Operating conditions

X-ray source current, 50 mA
X-ray source voltage, 120 kV
32 sequential images in single scan
Thickness of sample covered by
1 sequential image, 0.625 mm

XCT images of cores

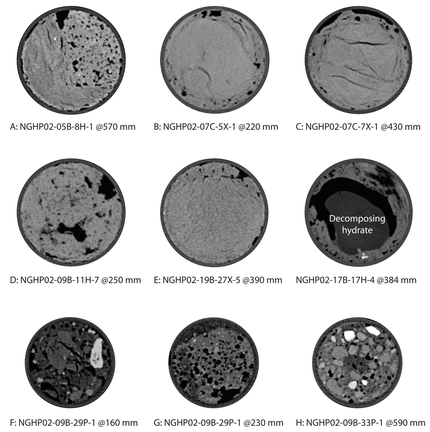

Examples of voxel data obtained from the XCT measurement of core sections (ROI = Region of Interest; HU = Hounsfield Unit)

XCT image -->	A	B	C	D	E	F	G	H
Total number of voxel in ROI	111184	111201	111239	111562	111353	74502	74502	74613
Number of voxel with negative CT value	6443	2649	5418	11351	2110	5227	7486	1769
Number of voxel weighted	104592	108548	105819	100201	109226	65773	66887	67454
Minimum CT value in ROI (HU)	-1500	-1215	-1365	-1318	-1308	-1395	-1446	-1498
Maximum CT value in ROI (HU)	4193	1586	1633	1680	3353	3625	2926	5058
CT value for weightage	2239	2339	2339	2464	2339	2314	2289	2264

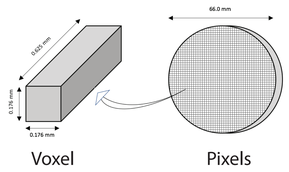

Concept

CT number for a known or assumed grain density (CT_G) is calculated by using density vs. CT calibration equation:

$CT_G = (\text{Grain density} - 0.9237) * 1250$

Frequency of voxels (V_X) corresponding to a measured CT number (CT_M) is converted to weighted frequency of voxels (V_W) as follows:

$V_W = [(CT_G - CT_M) / CT_G] * V_X$

Thus, frequencies of voxels with positive CT numbers closer to zero are assigned higher weightage than those closer to CT_G for their contribution to fluid fraction of sediments. Voxels with CT numbers same as CT_G or higher are not assigned any weightage, because they correspond to entirely solid material, and hence do not contribute to porosity. Finally, sum of all weighted frequencies of voxels (V_W) and frequencies of voxels with negative CT number ($CT_{M<0}$) is divided by sum of total number of voxels (V_{all}) in an XCT image to get the XCT based porosity value. The equation in this case can be written as:

$\text{Porosity} = (\Sigma V_W + \Sigma V_{CT(M<0)}) / \Sigma V_{all}$

Results

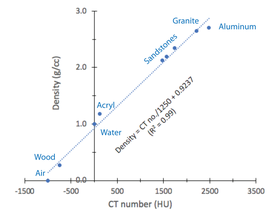

Calibration curve of the XCT (calibrated with air only on daily basis); error bars are smaller than the symbols at each data point

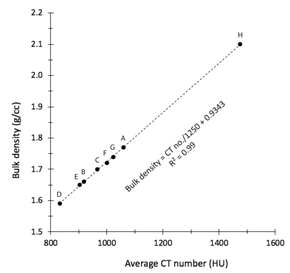

Bulk density of core material estimated by averaging CT numbers from 35 images of the core obtained by the XCT. Data labels correspond to the samples / images.

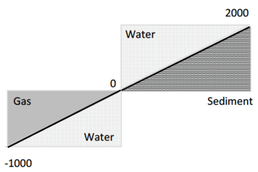

Schematic showing relative proportion of gas, water and sediment that determine CT number of a voxel

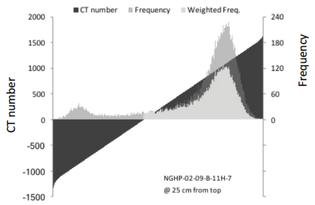

An example of CT number distribution of ca. 111,000 voxels in one XCT image

Slope of the calibration curve on the left (1/1250) is exactly same as that obtained by Ashi (1995), even though Ashi used totally different standards (6 bentonite samples having densities in the range 1.6 – 2.0 g/cc). This similarity of slope suggests that X-ray's response to density of target material is a constant. Linearity of the calibration curve ($R^2 > 0.93$) corroborates the point made by Akin and Kovscek (2003) that CT image (or CT number) is proportional to density of material being imaged, provided X-ray energy used is above 100 kV.

Average bulk densities estimated from average CT numbers show nearly same linearity in the data as that in the case of calibration curve (slope, 1/1250). Small difference in intercept (density) is likely to originate from much longer range of density (0 – 2.6 g/cc) used in calibration than that used in bulk density (1.6 – 2.2 g/cc) estimation.

Since the XCT imaging is done contiguously, porosity and density changes at resolution much higher than that obtained by the GRA and MAD techniques can be studied. Figure on the right shows variations in porosity and density over 2 cm thick interval of cores. Both parameters are strongly and inversely correlated with each other ($r < -0.9$) in all samples. Three cores (A, B, C) show minimum change over the 2 cm interval compared to that shown by the other cores. This indicates that the core material is quite homogenous within 2 cm interval of the 3 cores, while in other cores, heterogeneity of core material is obvious.

Porosities estimated from the XCT images are fairly close to those estimated by the MAD and GRA measurements. However, sandy material in some core samples yield much lower porosities probably due to collapse of voids (gas pockets) in sediments during the sampling process for MAD measurements. On the other hand, comparison of porosity values obtained from the XCT and GRA methods is reasonably good (high correlations), because these measurements are conducted on intact core material, prior to splitting it into archive and working halves.

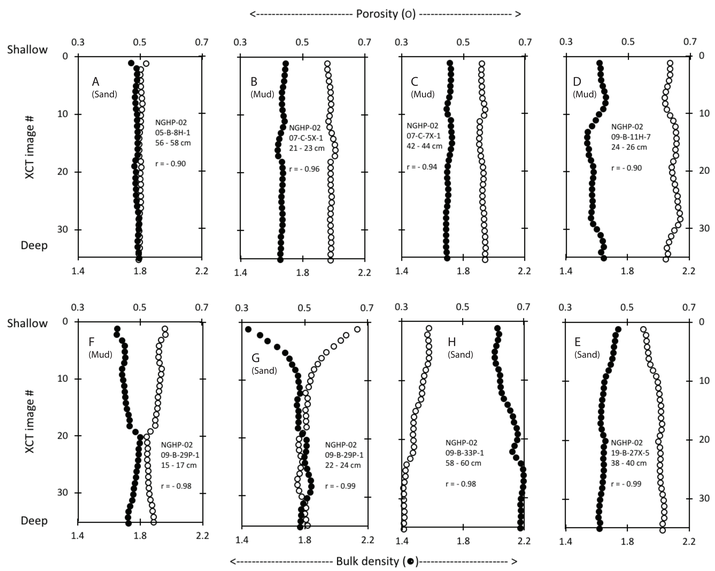

Variations in XCT based density and porosity data of the core samples with in 2 cm intervals that were sampled for estimation of these properties conventional MAD method.

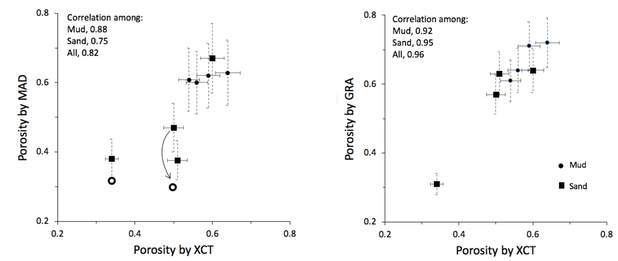

Comparison of error ranges in the porosity data obtained by various methods

Conclusion

With a priori knowledge of grain density of sediments, porosity of the sediments can be estimated soon after core recovery by using the XCT, while other methods take hours to make such estimates. Time is crucial in the case of hydrate-bearing sediments, because hydrate decompose rapidly due to change of ambient pressure and temperature, and thus affect bulk density and porosity of sediments.

Although gas, liquid and solid can co-exist in a space comparable or smaller than the size of a voxel, a binary system of fluid and solid only was considered in this study to keep the calculations simple. Micro-focus XCT can provide much higher resolution images to estimate relative proportions of gas, liquid and solids, but the sample size will become a limitation in this case. On the other hand, medical XCT scanner used in this study could scan the long cores (up to 150 cm long and 6.6 cm diameter). Therefore, it would not be wrong to state that medical XCT scanner is a powerful tool not only for visualization of hydrate, but also for on-site and quick characterization of physical properties like bulk density and porosity of sediments.

For more details, scan the QR code

References

Akin, S., Kovscek, A.R., 2003. Computed tomography in petroleum engineering research, in: Mees, F., Swennen, R., Van Geet, M., Jacobs, P. (Eds.), Application of X-ray Computed Tomography in the Geosciences. Special Publication - Geological Society of London, vol. 215, pp. 23-38.

Ashi, J., 1995. CT scan analysis of sediments from Leg 146, in: Carson, B., Westbrook, G.K., Musgrave, R.J., Suess, E. (Eds.), Proceedings of the Ocean Drilling Program, Scientific Results, Vol. 146 (Pt. 1), 191-199.

Acknowledgements

Authors are thankful to the Ministry of Petroleum & Natural Gas within the Government of India, Oil and Natural Gas Corporation Limited (ONGC), Directorate General of Hydrocarbons (DGH), Oil India Ltd, GAIL (India) Ltd, Indian Oil Corporation Ltd and all other NGHP partner organizations for providing the opportunity to contribute to the NGHP-02 Expedition and this special issue of the Journal of Marine and Petroleum Geology. The technical and science support from Japan Agency for Marine-Earth Science and Technology (JAMSTEC), United States Geological Survey (USGS), U.S. Department of Energy (US-DOE), the National Institute of Advanced Industrial Science and Technology (AIST), Geotek Coring and Schlumberger is gratefully acknowledged. Excellent technical and logistical support received on the drilling vessel D/V Chikyu was crucial to this research, which was funded by a special grant from the JAMSTEC for the NGHP-02 related studies.